Ligand Descriptor Analysis in Nickel-Catalysed Hydrocyanation: A Combined Experimental and Theoretical Study

Enrico Burello,[a] Philippe Marion,[b] Jean-Christophe Galland,[b] Alex Chamard,[b] Gadi Rothenberg[a,*]

[a] van't Hoff Institute of Molecular Sciences, University of Amsterdam, Nieuwe Achtergracht 166, 1018 WV Amsterdam, The Netherlands
Fax: (+31)-20-252-5604, e-mail: gadi@science.uva.nl
[b] Rhodia, Centre de Recherches de Lyon, 85, Rue des Frères Perret, BP62, 69192 Saint Fons Cedex, France

Received: November 26, 2004; Accepted: March 8, 2005

Abstract: The problem of choosing the 'right chelating ligand' for a homogeneously catalysed reaction is outlined. A model is introduced that combines mechanistic information and ligand descriptors. This model is used together with automated synthesis tools to study the structure-activity relationship in a diverse set of forty-two ligands, and extract information on active regions in the catalyst space. The concept is demonstrated on nickel-catalysed hydrocyanation, using bidentate phosphine and phosphite ligands. The charge at the ligating atoms, the rigidity of the molecules, the steric crowding around the Ni atom, and the bite angle are found to be the most important descriptors. A comparison is made with literature hydrocyanation data and approaches for designing new homogeneous catalysts are discussed.

Keywords: adiponitrile; combinatorial catalysis; data mining; homogeneous catalysis; molecular descriptors; QSAR

Introduction

Social and legislative demands for sustainable development in the 21st century is increasing the incentives for developing 'green' chemical processes. In many cases, this can be achieved by converting existing stoichiometric protocols into catalytic ones. The Metolachlor process[1] and the clean synthesis of Ibuprofen[2] are just two examples of the possible impact that homogeneous catalysis can have on the fine-chemical industry, providing that the right ligand/metal combination is found.

Unfortunately, that last proviso is much easier said than done. The problem of finding 'good' ligands is akin to searching for something in a haystack. It is not necessarily a needle, but it is small enough to rule out an exhaustive search of the catalyst space. This is true even when synthesis robots are used – it is impossible to synthesise and test all combinations.[3–5] It is possible, however, to narrow the search space using mechanistic information and structure/activity relationships (SARs).[6–12] A model can then be used to target these regions that contain, hopefully, the best catalysts. Feedback of experimental data into the model can enable an iterative search of the catalyst space.

Recently, we showed that by combining mechanistic information with molecular descriptors it is possible to build a model for Heck cross-coupling reactions catalysed by monodentate phosphine ligands.[11] This model was used to preselect candidates from large 'virtual libraries' of monodentate ligands.[13] In this paper, we extend the work to reactions catalysed by bidentate ligands, presenting descriptor models for nickel-catalysed hydrocyanation. We study the structure-activity relationship in a diverse set of ligands, and validate the model by comparing the results to existing mechanistic findings. As this model gives quantitative information, it can be used to indicate active regions in the catalyst space.

Results and Discussion

Choosing Descriptors for Chelating Ligands

Chelate-forming bidentate ligands participate in numerous types of homogeneous catalytic reactions, e.g., hydroformylation,[14] hydrocyanation,[15] peroxide decomposition,[16] and cross-coupling.[17] In most cases, fine-tuning of the ligands' steric and electronic properties is essential.[18] At first, it may seem that the number of variables that determines the activity of a ligand-metal complex is large, but in fact the catalytic properties of a bidentate ligand can be adequately described using a few well-chosen molecular descriptors.[19–21] It is important to emphasise that these descriptors should preferably represent physico-chemical characteristics that per-

 DOI: 10.1002/adsc.200404363

tain to mechanistic information (i.e., the descriptors should tally with 'chemical intuition'). For example, the complexation reaction of a ligand to a metal centre leads to the concept of bite angle.

We will consider bidentate ligands as assemblies of two parts: a backbone that connects the ligating atoms, and the R groups attached to these ligating atoms. We then divide the ligand descriptors into three classes:

a) chelating effect-related descriptors that provide information about the size, flexibility and conformational changes of the ligand upon complexation with the metal;
b) steric descriptors that pertain to the shape of the ligands and the substrate accessibility to the metal centre; and
c) electronic descriptors that measure the charge distribution and the orbital energies at the ligating atoms.

Descriptors Related to the Chelating Effect

The bite angle[22] (α) was one of the first parameters employed to show a structure-activity correlation of chelating ligands in homogeneous catalysis.[23–26] This descriptor calculates the angle between the metal and the two ligating atoms. Its value is a compromise between the ligands' preferred bite angle and the type and number of *d* orbitals available from the metal (Figure 1, top).

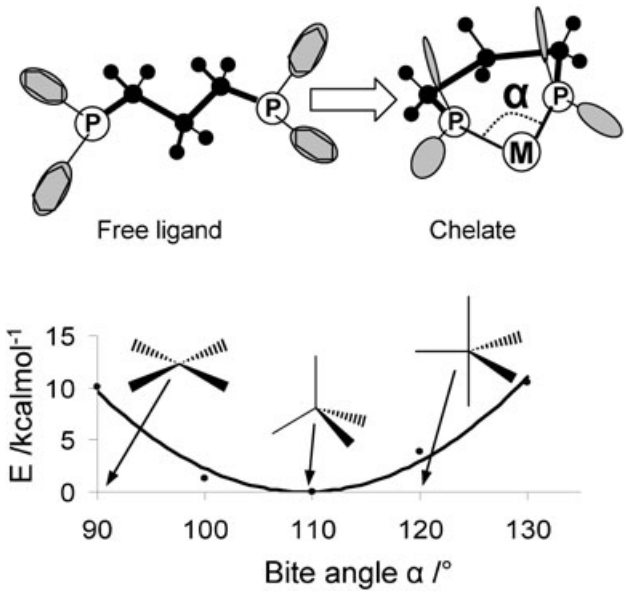

Figure 1. (*Top*): The bite angle (α) is the angle formed when a bidentate ligand coordinates to a metal centre; (*bottom*) A flexibility profile showing the energy change *vs.* the bite angle (a second degree polynomial function). In this example, square planar co-ordination structures ($\alpha = 90^\circ$) are disfavoured (10 kcal above the minimum). Tetrahedral and trigonal bipyramidal structures are closer to the minimum and therefore more likely to occur.

The bite angle varies during the catalytic cycle, as confirmed by many mechanistic studies – a 'good ligand' is one that can support the metal throughout the cycle, preventing the elimination pathways. As ligands can adopt geometries with energies slightly above that of the minimised structures, we introduce a second variable that measures the range of bite angle accessibility (Figure 1, *bottom*). This flexibility parameter, *a*, is calculated by fixing the bite angle of ligands to standard values (90°, 100°, 110°, 120° and 130°) and minimising the constrained structures. The result is a parabolic energy potential that depends on the bite angle. The flexibility *a* is the second derivative of this polynomial.

We use two descriptors to account for the changes that result from the ligand/metal binding: ΔE_{bind} is the energy difference between the 'free ligand' and the complex, and Δd is the difference in the inter-atomic distance between the ligating atoms between the 'free ligand' and the complex. These two descriptors reveal to what extent a ligand adopts a chelating conformation before binding to the metal.

Steric Descriptors

This class includes descriptors such as the molecular volume (*V*) and surface (*S*) which are commonly used to characterise the shape of ligands, as well as the cone angle (Θ),[27,28] and the sphere occupation (S_{occ}).[29–31] This last descriptor gives the free accessible space left by a ligand after complexation with a metal centre and estimates the ability of that complex to coordinate an additional substrate (e.g., during an oxidative addition step). It is related to the size of the 'reaction pocket'.

We also calculated the solid angle, the radius at the ligand's maximal solid angle and related properties.[29–31] These descriptors were calculated both for the backbone and the ligand structures (a full list of the descriptors is given in Table 1 in the Experimental Section).

Electronic Descriptors

Several studies were performed to separate the electronic and the steric effect of ligands.[32] Spectroscopic values and pK_a values of phosphines are examples of frequently employed parameters. Here we used the charges of ligating atoms and the HOMO, LUMO and enthalpy of formation energies (calculated using PM3 semi-empirical methods, *vide infra*) as well as dipole moments. The Mulliken and the electrostatic charges were also calculated for both ligating atoms at the 'free ligand' and at the complex conformations.

An Experimental Example: Catalytic Hydrocyanation of 4-Pentenenitrile

The nickel-catalysed hydrocyanation of pentenenitrile [Eqs. (1)–(5)] is one of the best examples of homogeneous catalysis on an industrial scale.[15,18,33–35] Scheme 1 shows a simplified mechanism for the hydrocyanation of pentenenitrile using bidentate ligand Ni complexes, analogous to the one proposed by Freixa and van Leeuwen for the case of styrene.[24]

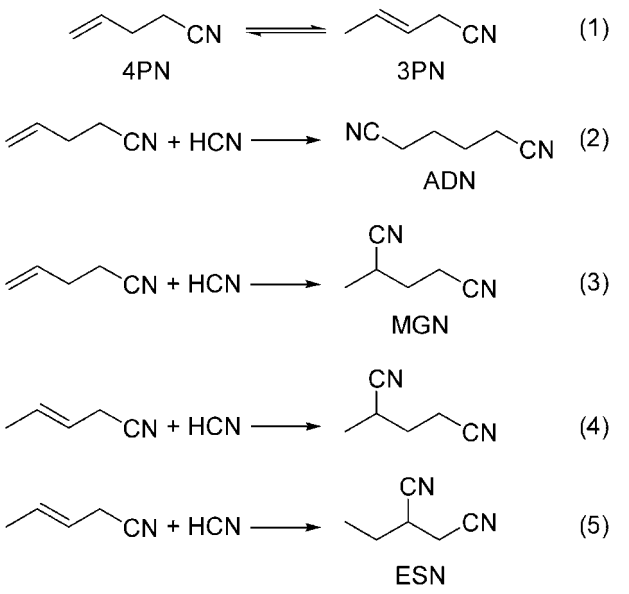

In this mechanism, the catalyst precursor **1** binds a bidentate ligand to enter the catalytic cycle. It undergoes both an oxidative addition with HCN and an olefin insertion with 4PN to yield intermediate **4**. Olefin reduction leads to structure **5**, which then eliminates the dinitrile product, generating species **2** (or **3**) and completing the catalytic cycle. Intermediates are stabilised by P–Ni–P bite angles of 120° (in trigonal compounds), 109° [in the tetrahedral Ni(0) species], and 90° for the allyl, alkyl or hydrido cyano Ni(II) complexes.

Using a parallel reactor system, we screened 42 bidentate ligands in a search for the optimal linear:branched hydrocyanation product ratio ADN:(MGN + ESN). A selection of these ligand structures is shown below (structures **6**–**21**). Most of the ligands employed in this study are commercially available and represent a diverse set of structures that include biphosphines, biphosphites and {P,N,S} ligands. When one has to start almost at point zero, it is preferable to include as many ligand families as possible. This is done both to sample different catalyst options as well as to obtain a model that is able to screen a broad range of structural variations. For all the ligands we calculated a total of 39 chelating, steric, and electronic descriptors (Table 1). The calculation yields the model input, a two-dimensional matrix where each row corresponds to an observable (a ligand) and each column is a descriptor. From the experimental results we obtain the figure of merit (in this case, % yield of the desired product, ADN). Yield values range from a minimum of 0% to a maximum of 72% conversion. The

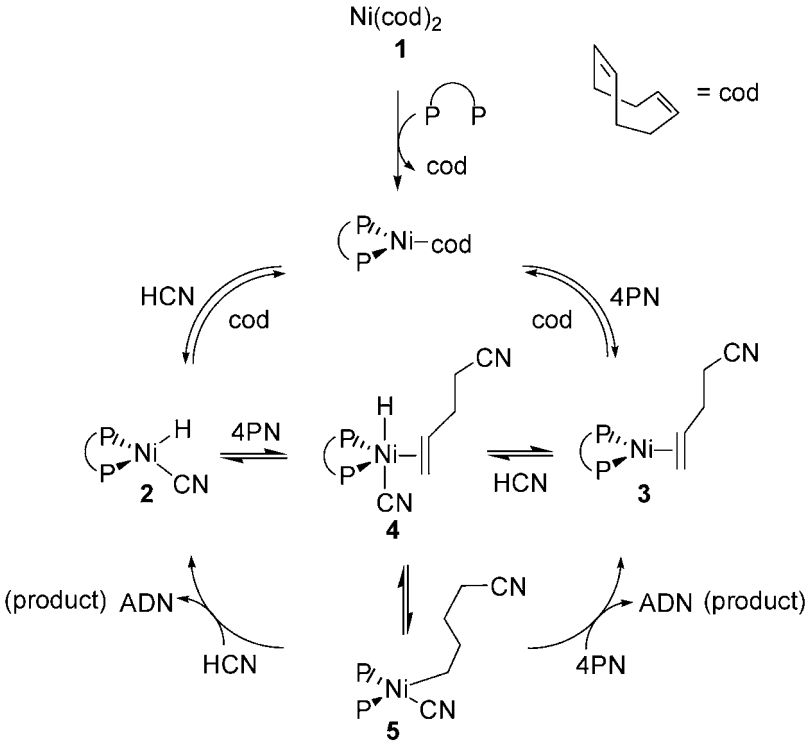

Scheme 1. Catalytic cycle for pentenenitrile hydrocyanation.

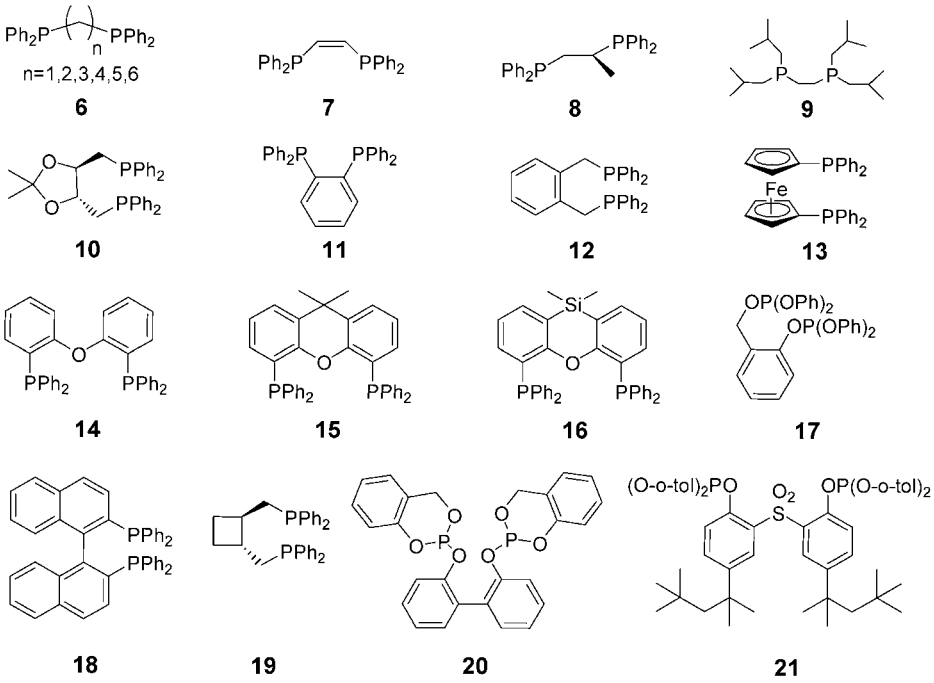

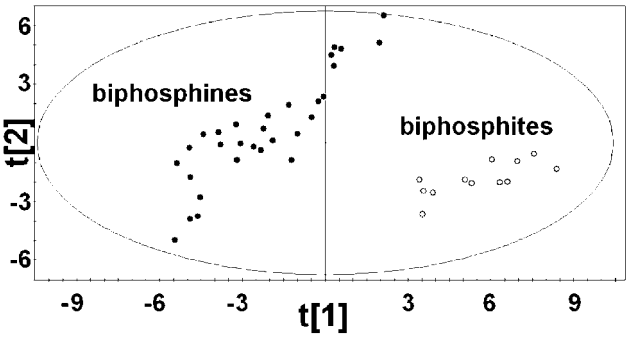

Figure 2. Score plot of bidentate ligands. Compounds are plotted in the first two principal components, which retain 61% of the information contained in the original descriptors ($R^2 = 0.61$). The ligands cluster into biphosphine and biphosphite structures (some N and S ligands are included in the first group). The clustering reflects different charge and steric properties between the two classes.

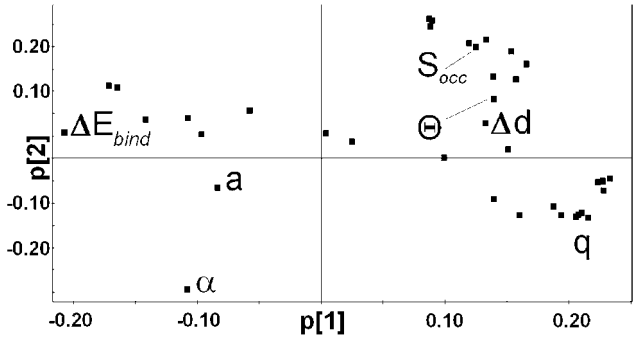

Figure 3. Descriptors loadings plot. This plot shows the degree of correlation between descriptors. Charge (q) and steric descriptors are clustered, while the other descriptors are more scattered (i.e., uncorrelated).

standard deviation and the average values in the dataset are 16.3 and 9.6, respectively. Two-thirds of the reactions resulted in a poor yield (0–10%), and only three ligands gave >50% yield.

We then used principle components analysis (PCA) to reduce the rank of the problem. PCA creates an irreducible "ligand profile", a minimal representation of the structural changes among the set of ligands. Using 2, 4, and 8 PCs we could explain 61%, 83%, and 99% of the variance in the data, respectively. Figure 2 shows the ligand representation using the first two principal components as axes (cumulative variation $R^2 = 61\%$). Two clusters are observed, reflecting the type of compounds analysed: biphosphines and biphosphites (the biphosphines group includes also some N and S ligands). The descriptors that influence most this type of clustering are the charge at the ligating atoms and the sterics of the molecules as shown in Figure 3, where a correlation structure between properties is given by plotting the variable loadings of the first two principal components. We observe clusters for some descriptors, such as the charge and the steric ones. Others, e.g., the bite angle, the flexibility and the HOMO and LUMO energies are more scattered.

From these correlations we see that bidentate ligands can be represented by a reduced set of dimensions, the characterisation of which requires minimal information. Moreover, the score plot in Figure 2 indicates the com-

pound's position in the catalyst space and estimates the degree of similarity between them. In other words, each time you introduce a new ligand, you can see which direction you are taking in the catalyst space.

Variable Importance (VIP) Studies

The structure-activity correlation determined using PLS regression analysis results in a two-component model. The gross statistical performances of a PLS model can be deduced from the parameters R^2 (the goodness of fit or explained y-variation) and Q^2 (the predicted y-variation). Our model gives $R^2 = 0.850$, and $Q^2 = 0.785$. There is evidently a good correlation between some of the descriptors and the yield. To identify which descriptors (i.e., which properties of the ligands) have a strong effect on the catalytic activity, we plotted the contribution of each descriptor to the model (Figure 4).

We see that the most important variables are the electrostatic and the Mulliken charges at the ligating atoms. These electronic properties are known to influence the complex's stability and the elementary steps of the catalytic cycle.[14,18,24] Ligands with electron-withdrawing substituents at the phosphorus atoms are weak bases and can easily compensate the high electron density of the d^{10} zerovalent nickel by back-donation. An electron-poor nickel atom will readily coordinate the olefin substrate. Moreover, kinetic studies[36] indicate that the rate of reductive elimination (the rate-limiting step) is increased by electron-withdrawing ligands such as phosphites. The order of activity found in our dataset was: $NR_3 < SR_2 \ll PR_3 < P(OR)_3$.

The first steric property found to influence activity is a chelating effect-related descriptor: the energy difference between the free and the coordinated conformation of ligands (ΔE_{bind}). The model selects ligands where only few structural arrangements are necessary to form a chelate complex. This requirement reflects the need

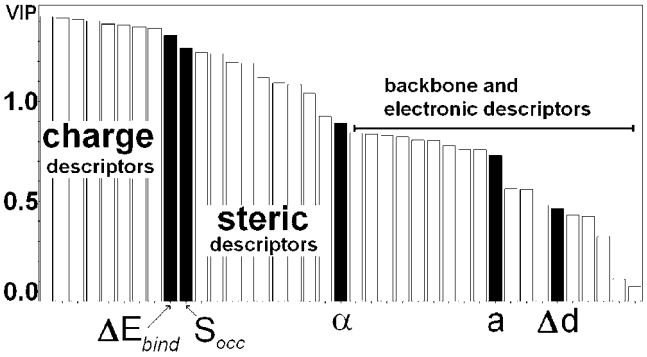

Figure 4. Variable importance (VIP) plot, showing the importance of every variable in the model. The solid columns denote the descriptors highlighted in Figure 3. VIP values higher than 1.0 are attributed to descriptors that contribute most in the prediction of ligands activity.

for highly stable complexes during the catalytic cycle and confirms experimental findings which show that rigid and large bidentate ligands are effective in catalytic hydrocyanation.[14] Compounds with rigid backbones, such as the Xantphos-type ligands **14**–**16**, where the donor atoms are well oriented to form the metal complex, induce small variations in the bite angle and therefore adopt the desired binding mode. When phosphites are used, the additional oxygens increase the flexibility of the backbone and with it the chance of "losing" the optimal orientation. This effect can be avoided by tuning the interactions between the R groups and the backbone and/or by omitting the oxygens that bind the phosphorus to the backbone structure.

The third-ranked variable is the sphere occupation descriptor (S_{occ}), a measure of the steric crowding around the nickel atom. Ligand-metal complexes with S_{occ} values of 70–80% are found to be the most active. These ligands are able to coordinate the other reagents (the proton, the cyanide and the olefin) that contribute little to the steric crowding. Moreover, S_{occ} is correlated better with the cone angle Θ ($R^2 = 0.65$), than with the bite angle α ($R^2 = 0.31$, see score plot in Figure 3). This difference reflects the fact that calculations of S_{occ} and Θ take into account also the R group steric effect, while α is mainly a measure of the backbone structure. The R groups affect the accessibility of other substrates to the metal centre and "push" the reagents together to favour the coupling process during the elimination step.[36] S_{occ} can therefore be considered as an indicator of such R group effects. Ligands with *ortho* substituents on the phenyl rings (e.g., **21**) increase the steric crowding at the metal centre, with a strong influence on the catalytic activity. Such cases would favour a reaction with 4PN over 3PN, as the former is less hindered and thus has a better chance to coordinate to the Ni atom. For the same reason, the formation of the linear product ADN is also preferred over that of the bulkier MGN and ESN isomers.

The group of steric variables and the bite angle (α) form the last group of important parameters that affect the catalytic activity. The bite angle indicates a peak of activity around 105°–110°, which explains why large biphosphines that stabilise the tetrahedral complexes also enhance the reductive elimination step.[24] Conversely, small bite angle ligands (e.g., dppe or dppp), stabilise square planar geometries, accelerating the deactivation pathways and thus forming Ni(II) complexes such as $Ni(L)_2(CN)_2$. The remaining descriptors (backbone structural parameters, HOMO and LUMO energies, dipole moments, etc.) are not so relevant to this model.

Although the first homogeneously catalysed hydrocyanation of linear alkenes was published in 1954 by Arthur and co-workers,[37] only a few more examples representing this class of substrates can be found in the literature. In the last ten years, the Xantphos ligand and several of its structural variations have been extensively

studied in the hydrocyanation of 1-octene, styrene and ω-unsaturated fatty acid esters. A direct comparison between the catalytic activities of the ligands tested in this study and the Xantphos-type compounds presented in the previous works is not possible, as the starting material used in our study (pentenenitrile) differs from those used in the literature. To overcome this problem we included in our library several Xantphos-type ligands and modelled them. These ligands showed moderate activity (less than 30% conversion) in the hydrocyanation of pentenenitrile, destabilising the square-planar geometry of the divalent state and stabilising the tetrahedral geometry of the zerovalent state by means of a wider bite angle.

Another approach to design better catalysts is to enhance the reductive elimination rate. Biphosphites have proven to be versatile ligands in this case, as the reaction is facilitated by electron-withdrawing ligands. Biphosphites containing aryl groups and having wide bite angles combine the two effects, and make good catalysts (the ligands used by Casalnuovo et al.[38] are designed to combine these two features using glucose backbones and trifluoromethyl groups at the *meta*-position in the PPh moieties). Indeed, in our work, the ligands that gave the highest conversion (e.g., compound **21**) also displayed both characteristics: a rather rigid and large backbone, and electron-withdrawing ligating atoms.

Although the bite angle and electronic effects seem reasonable, an increasing steric crowding around the nickel atom might also enforce the reductive elimination step. Freixa and van Leeuwen evidenced this argument for the methoxycarbonylation reaction of alkenes with palladium catalysts, where it was shown that steric bulk is more important than the bite angle.[24] We also find that the presence of bulky substituents on the P atoms enhances the conversion of pentenenitrile by increasing the steric crowding around the nickel atom. We believe this feature (encoded by the S_{occ} descriptor) is another way to control the catalytic activity of ligands in pentenenitrile hydrocyanation.

Conclusions

The brute force approach to bidentate ligand optimisation is hampered by the huge diversity of the multi-dimensional ligand space. A complete search is not possible, and even a partial search is likely to require the synthesis and testing of large numbers of compounds with hardly any activity. One way to overcome this problem is to use predictive models to preselect 'good regions' of the catalyst space and search there for ligands. Focusing on the catalytic hydrocyanation of pentenenitrile, we derived a QSAR (multivariate) model that correlates the ligands' activities with their structural and electronic properties. The choice of targeted descriptors (i.e., related to the reaction) is the first step in order to get a model that could then be interpreted in terms of mechanistic arguments. The charge at the ligating atoms, the rigidity of the molecules, the steric crowding around the Ni atom and the bite angle are found to be the most important descriptors. In this way the model provides a rational and quantitative way to screen virtual libraries of ligands in search of new hydrocyanation catalysts. This combination of synthesis and *in silico* screening will be the subject of future work in our laboratory.

Experimental Section

Materials and Instrumentation

Reactions were performed in a glove box under an inert atmosphere using a Gilson 215 automated robot platform equipped with two sampling syringes and modified to enable orbital stirring and temperature control.[39] The temperature homogeneity in each well was $\pm 1\,^{\circ}C$. GC analyses were performed using a Varian CP 7331 gas chromatograph with a 100 μm × 10 m capillary column. All chemicals were purchased from commercial sources (>99% pure) and used as received. All products are known compounds and were identified by comparison of their spectral properties and GC retention times to those of commercial samples. Lewis acids were diluted in DMF to 1.5 M concentration and filtered prior to reaction.

Procedure for Catalytic Hydrocyanation of 4-Pentenenitrile

The catalyst precursor $Ni(COD)_2$ (10 μmol, 2.7 mg), ligand (50 μmol for monodentate and 100 μmol for bidentate ligands), 3-pentenenitrile (300 μmol, 24.3 mg), Lewis acid stock solution (10 μmol, 0.67 μL), cyanohydrin (300 μmol, 8.1 mg), diisopropylbenzene (2 mg, internal standard) and DMF (2000 μmol, 146.2 mg) were added to 3-mL reaction vials. These were sonicated for 20 min and subsequently heated to 70 °C. After 2 h stirring, the vials were cooled to 25 °C, and the reaction mixtures were diluted with DMF and analysed by GC.

Computational Methods

A detailed description of the use of the principal component analysis (PCA) and partial least squares (PLS) analysis methods in the assessment of virtual ligand libraries was recently published for monodentate palladium-phosphine ligands.[11]

Here we introduce an additional parameter, the variable importance (VIP), to estimate the contribution of each descriptor in the PLS model. PLS modelling is a simultaneous projection of the variables matrix **X** and the figures of merit matrix **Y** on lower-dimensional hyper-planes. The coordinates of the points in these hyper-planes are the elements of the low-rank matrices **T** and **U**. The PLS algorithm uses additional loadings, w, (also called weights) to express the correlation between **U** and **X**. This analysis has two objectives: *(a)* to reduce the dimensionality of the problem and still give a good approximation of the **X**

and **Y** spaces; and *(b)* to maximise the correlation between **X** and **Y**.

We used cross-validation to determine the model dimensionality (number of principal components). A component n is considered significant if the value PRESS/SS is smaller than 1, where PRESS is the sum of square differences between observed and predicted Y values when observations are kept out, and SS is the residual sum of squares of component $(n-1)$.

Assessment of Variable Importance (VIP)

The influence of each descriptor on the figure of merit is calculated as the VIP parameter. This is the sum over all model dimensions of the VIN (variable influence) contributions. For a given descriptor k and a given PLS dimension a, $(VIN_{ak})^2$ is equal to the squared PLS weight $(w_{ak})^2$ of that term, multiplied by the SS explained by that PLS dimension. The accumulated value VIP_k [Eq. (6)] is then divided by the total percentage of explained variance and multiplied by the number of terms in the model. A descriptor with $VIP_k > 1$ is considered as relevant to the model.

$$VIP_k = \sum_a (VIN)_k^2 \qquad (6)$$

Molecular Geometry optimization

Molecular Mechanics and semi-empirical PM3 methods[40] within the Spartan program[41] were used to optimise the geometries of ligands. The structures obtained were then used as the starting point for the calculation of all descriptors (see Table 1). The Steric programme[42] was employed to calculate the solid angle of ligands and related properties.

An important issue that drives the selection of descriptors is the level of theory used in the calculations. In combinatorial chemistry this choice is mainly influenced by the size and molecular complexity of the libraries and the computing time available. When you have to handle large libraries, simple and efficient rules that enable a rapid selection of structures are the only applicable solution. Molecular modelling force fields are a fast and precise tool for obtaining ligand geometries.[43] These programmes give good results and offer the advantage of performing data analysis on molecules before they are synthesised. Moreover, to validate our calculations, the bite angles of known ligands were compared with their crystallographic data deposited at the Cambridge Crystallographic Database and with other molecular modelling results performed elsewhere.[22] The trends we observed were in good agreement with both controls.

Table 1. Molecular descriptors used to characterize ligand structures.[a]

Entry	Symbol	Description	Min.	Max.	Mean	Std. Dev.
Chelating effect descriptors						
1	α	Bite angle [degrees]	74.2	127.7	107.3	10.7
2	a	Flexibility [(kcal mol^{-1}degrees^{-2})]	0.012	0.044	0.025	0.008
3	ΔE_{bind}	Free-Chelate conformation energy difference [kcal mol^{-1}]	16.9	96.0	42.9	18.5
4	Δd	Free-Chelate conformation distance difference [Å]	0.19	4.35	2.06	1.13
5	$d_{(P1-P2)}$[e]	Ligating atoms distance, free conformation [Å]	3.10	8.05	5.69	1.24
6	$d_{(P1-P2)c}$	Ligating atoms distance, chelate conformation [Å]	3.10	8.05	5.69	1.24
Steric descriptors						
7[b]	Mw	Molecular weight [amu]	226	987	549	190
8[b, c]	S	Van der Waals surface [Å^2]	258	988	587	173
9[b, c]	V	Volume enclosed in van der Waals surface [Å^3]	242	1051	584	188
10	d_{PATH}	Sum of bond distances between ligating atoms[e] [Å]	3.7	12.6	9.2	2.3
11[b]	Θ	Tolman's cone angle [rad]	4.06	6.93	5.87	0.67
12[b]	Ω_{max}	Maximum numerical solid angle [sr]	4.8	12.2	8.0	2.3
13[b]	S_{occ}	Percentage of sphere occupation [%]	38.0	87.0	64.5	18.6
14[b]	A_{sap}	Area under numerical solid angle profile [Åsr]	14.8	57.9	37.7	12.6
15[b]	R_{max}	Radius at numerical solid angle profile peak [Å]	2.75	6.42	3.97	1.14
Electronic descriptors						
16[c]	E_{HOMO}	HOMO [eV]	−8.68	−6.99	−7.72	0.50
17[c]	E_{LUMO}	LUMO [eV]	−1.22	0.94	−0.13	0.42
18[c]	GAP	$E_{LUMO}-E_{HOMO}$ [eV]	6.54	8.47	7.60	0.46
19[c]	μ	Dipole moment [Debye]	0.41	8.73	2.56	2.19
20[c, d]	$q_{1,P}$	Electrostatic potential on P atom [kcal mol^{-1}]	0.01	1.28	0.72	0.38
21[c, d]	$q_{2,P}$	Mulliken charge on P atom [e]	−0.03	1.29	0.67	0.42

[a] Some descriptors were computed more than once, e.g., the volume was computed both for the complete ligand and for the backbone.
[b] Calculated also for the backbone structure.
[c] Calculated for both the free and the chelating conformations. The statistics refer to the chelating conformation only.
[d] Averaged charge values between the two ligating atoms were also computed.
[e] The distance was calculated considering the minimum bonding path distance between P_1 and P_2 ligating atoms.

References and Notes

[1] Metolachlor is an *N*-chloroacetylated, *N*-alkoxyalkylated, *ortho*-disubstituted aniline that has both a chiral axis and a stereogenic centre. The current manufacturing process, by Ciba-Geigy/Novartis, is one of the most active and productive enantioselective catalytic systems ever developed. For a general review, see: R. R. Bader, H.-U. Blaser, *Stud. Surf. Sci. Catal.* **1997**, *108*, 17; for "A Personal Account" of this work, see: H.-U. Blaser, *Adv. Synth. Catal.* **2002**, *344*, 17.

[2] Ibuprofen is a non-steroidal anti-inflammatory painkiller (known also as Advil™ or Motrin™). The new manufacturing process commercialised in 1992 by BHC involves only three catalytic steps, with >80% percent atom economy, and up to 99% when including the recovered AcOH by-product. This process replaces six stoichiometric steps and improves atom economy by 60%. A detailed description is available on http://www.epa.gov/greenchemistry/aspa97.html.

[3] O. Lavastre, *Actual. Chim.* **2000**, 42.

[4] A. Hagemeyer, B. Jandeleit, Y. M. Liu, D. M. Poojary, H. W. Turner, A. F. Volpe, W. H. Weinberg, *Appl. Catal. A: Gen.* **2001**, *221*, 23.

[5] S. Dahmen, S. Brase, *Synthesis* **2001**, 1431.

[6] A. L. Fernandez, C. Reyes, A. Prock, W. P. Giering, *J. Chem. Soc. Perkin Trans. 2* **2000**, 1033.

[7] A. L. Fernandez, M. R. Wilson, A. Prock, W. P. Giering, *Organometallics* **2001**, *20*, 3429.

[8] S. Wold, M. Sjostrom, L. Eriksson, *Chemom. Intell. Lab. Sys.* **2001**, *58*, 109.

[9] L. Eriksson, M. Sjostrom, S. Wold, *J. Chemom.* **1996**, *10*, 77.

[10] L. Eriksson, E. Johansson, *Chemom. Intell. Lab. Sys.* **1996**, *34*, 1.

[11] E. Burello, G. Rothenberg, *Adv. Synth. Catal.* **2003**, *345*, 1334.

[12] C. Reyes, A. Prock, W. P. Giering, *J. Organomet. Chem.* **2003**, *671*, 13.

[13] E. Burello, D. Farrusseng, G. Rothenberg, *Adv. Synth. Catal.* **2004**, *346*, 1845.

[14] P. C. J. Kamer, P. W. N. M. van Leeuwen, J. N. H. Reek, *Acc. Chem. Res.* **2001**, *34*, 895.

[15] M. Kranenburg, P. C. J. Kamer, P. W. N. M. Van Leeuwen, D. Vogt, W. Keim, *J. Chem. Soc. Chem. Commun.* **1995**, 2177.

[16] G. Rothenberg, H. Wiener, Y. Sasson, *J. Mol. Catal. A: Chem.* **1998**, *136*, 253.

[17] M. Kranenburg, P. C. J. Kamer, P. W. N. M. van Leeuwen, *Eur. J. Inorg. Chem.* **1998**, 155.

[18] W. Goertz, W. Keim, D. Vogt, U. Englert, M. D. K. Boele, L. A. van der Veen, P. C. J. Kamer, P. W. N. M. Van Leeuwen, *J. Chem. Soc. Dalton Trans.* **1998**, 2981.

[19] A. Fernandez, C. Reyes, T. Y. Lee, A. Prock, W. P. Giering, C. M. Haar, S. P. Nolan, *J. Chem. Soc. Perkin Trans. 2* **2000**, 1349.

[20] D. Woska, A. Prock, W. P. Giering, *Organometallics* **2000**, *19*, 4629.

[21] M. R. Wilson, A. Prock, W. P. Giering, A. L. Fernandez, C. M. Haar, S. P. Nolan, B. M. Foxman, *Organometallics* **2002**, *21*, 2758.

[22] P. Dierkes, P. W. N. M. Van Leeuwen, *J. Chem. Soc. Dalton Trans.* **1999**, 1519.

[23] P. C. J. Kamer, J. N. H. Reek, P. W. N. M. van Leeuwen, *Chemtech* **1998**, *28*, 27.

[24] Z. Freixa, P. W. N. M. van Leeuwen, *J. Chem. Soc. Dalton Trans.* **2003**, 1890.

[25] P. W. N. M. van Leeuwen, P. C. J. Kamer, J. N. H. Reek, *Pure Appl. Chem.* **1999**, *71*, 1443.

[26] P. W. N. M. van Leeuwen, P. C. J. Kamer, L. A. van der Veen, J. N. H. Reek, *Chin. J. Chem.* **2001**, *19*, 1.

[27] C. A. Tolman, *Chem. Rev.* **1977**, *77*, 313.

[28] T. L. Brown, K. J. Lee, *Coord. Chem. Rev.* **1993**, *128*, 89.

[29] D. White, B. C. Taverner, P. G. L. Leach, N. J. Coville, *J. Comp. Chem.* **1993**, *14*, 1042.

[30] D. White, B. C. Tavener, P. G. L. Leach, N. J. Coville, *J. Organomet. Chem.* **1994**, *478*, 205.

[31] B. C. Taverner, J. M. Smith, D. P. White, N. J. Coville, *South Afr. J. Chem.* **1997**, *50*, 59.

[32] L. Perrin, E. Clot, O. Eisenstein, J. Loch, R. Crabtree, *Inorg. Chem.* **2001**, *40*, 5806.

[33] W. Goertz, P. C. J. Kamer, P. W. N. M. van Leeuwen, D. Vogt, *Chem. Commun.* **1997**, 1521.

[34] J. D. Druliner, *Organometallics* **1984**, *3*, 205.

[35] J. E. B. A. S. Andell, *Organometallics* **1986**, *5*, 2350.

[36] J. E. Marcone, K. G. Moloy, *J. Am. Chem. Soc.* **1998**, *120*, 8527.

[37] P. Arthur, Jr., D. C. England, B. C. Pratt, G. M. Whitman, *J. Am. Chem. Soc.* **1954**, *76*, 5364.

[38] A. L. Casalnuovo, T. V. RajanBabu, T. A. Ayers, T. H. Warren, *J. Am. Chem. Soc.* **1994**, *116*, 9869.

[39] J. M. Serra, A. Corma, D. Farrusseng, L. Baumes, C. Mirodatos, C. Flego, C. Perego, *Catalysis Today* **2003**, *81*, 425.

[40] For a discussion on the relative merits of semi-empirical methods, see: N. T. Anh, G. Frison, A. Solladie-Cavallo, P. Metzner, *Tetrahedron* **1998**, *54*, 12841.

[41] Spartan is distributed by Wavefunction Inc., 18401 Von Karman Ave., #370, Irvine, CA 92612, USA.

[42] Copyright 1994, C. T. Steric, all rights reserved.

[43] K. J. Lee, T. L. Brown, *Inorg. Chem.* **1992**, *31*, 289.

